JACS
JOURNAL OF THE AMERICAN CHEMICAL SOCIETY

Article

Self-Assembled Pd(II) Barrels as Containers for Transient Merocyanine form and Reverse Thermochromism of Spiropyran

Prodip Howlader, Bijnaneswar Mondal, Prioti Choudhury Purba, Ennio Zangrando, and Partha Sarathi Mukherjee

J. Am. Chem. Soc., **Just Accepted Manuscript** • DOI: 10.1021/jacs.8b03946 • Publication Date (Web): 06 Jun 2018

Just Accepted

ACS Publications

is published by the American Chemical Society. 1155 Sixteenth Street N.W., Washington, DC 20036

Self-Assembled Pd(II) Barrels as Containers for Transient Merocyanine form and Reverse Thermochromism of Spiropyran

Prodip Howlader,[a] Bijnaneswar Mondal,[a] Prioti Choudhury Purba,[a] Ennio Zangrando[b] and Partha Sarathi Mukherjee[a]*

[a] Department of Inorganic and Physical Chemistry, Indian Institute of Science, Bangalore 560012, India

[b] Department of Chemical and Pharmaceutical Sciences, University of Trieste, 34127 Italy.

ABSTRACT: Self-assembly of a *cis*-blocked Pd(II) 90° ditopic acceptor [*cis*-(tmeda)Pd(NO_3)$_2$] (**M**) with a tetradentate donor **L**[1] [benzene-1,4-di(4-terpyridine)] in 2:1 molar ratio yielded two isometric molecular barrels **MB1** and **MB3** in DMSO [tmeda = N,N,N′N′-tetramethylethane-1,2-diamine]. Exclusive formation of the symmetrical tetrafacial barrel (**MB1**) was achieved when the self-assembly was performed in aqueous medium. The presence of a large confined cavity makes **MB1** as a potential molecular container. Spiropyran (**SP**) compounds exist in stable closed spiro-form in visible light and converts to transient open merocyanine (**MC**) form upon irradiation with UV-light or upon strong heating. The transient **MC** form readily converts to the stable closed **SP** form in visible light. **MB1** has been employed as a safe container to store the planar and unstable merocyanine isomers (**MC1/2**) of different spiropyran molecules (**SP1/2**) [**SP1/2** = 6-bromo-spiropyran and 6-nitrospiropyran] for several days. The transient **MC** forms (**MC1** and **MC2**) were found to be stable inside the molecular container **MB1** under visible light and even in presence of different stimuli such as heat and UV-light for long time. Such stabilization of **MC** forms inside the confined cavity of **MB1** is noteworthy. This phenomenon was generalized by utilizing a carbazole based molecular barrel (**MB2**) as a host, which also showed a similar stabilization of transient **MC** form in visible light at room temperature. Moreover, reverse thermochromism was observed as a result of heating of the **MC1⊂MB2** complex, which de-encapsulates the guest in the form of **SP1** to give a colourless solution. Moreover, both the host molecules (**MB1, MB2**) were capable of stabilizing transient **MC2** even in solid state. Such stabilization of transient **MC** forms in solid state and transformation of **SP** forms to **MC** forms in solid state in presence of molecular barrel are remarkable; and these properties have been employed in developing a magic ink.

Introduction

Chemists have been inspired by Nature with its ample repository of dynamic chemical systems in the biological processes such as heat and touch response in plants/bacteria; animal camouflage[1] and retinal in visual excitation[2] etc. where molecules can change their structures reversibly under various external stimuli such as light, pressure, temperature.[3-6] Such dynamic materials have potential applications in molecular devices like molecular wires, sensors, switches, logic gates, signal nanoprocessors etc.[4] Among these, photo-induced switches are the most studied systems in recent years because of the numerous advantages of light as it can deliver high spatial and temporal precision.[4d,4e,5] Consequently, several photoswitchable molecules like azobenzenes, stilbenes, spiropyrans, diarylethenes etc. have been investigated in order to construct photo-responsive smart materials.[6] Nonetheless, spiropyrans are one of the most inimitable examples of photo-switches, whose closed-ring stable isomer (**SP**) converts into a highly polar, open-ring metastable merocyanine (**MC**) isomer by cleaving C_{spiro}-O bond upon exposure to UV light.[7] These two switchable isomers have vastly different properties and the range of stimuli that induces this switching between isomers include temperature, pH, redox potential, metal ions, mechanical force etc.[8] The stable **SP** form has a non-planar geometry whereas the metastable form **MC** acquires a planar Zwitterionic structure. This difference in shape and polarity changes the fate of stability of such isomers in different solvents, solid matrix, gels, molecular hosts etc.[9]

The evolution of coordination-driven self-assembly[10] in the past two decades has enabled chemists to develop many 3D molecular architectures having defined nanocavities.[11] Many of these molecular architectures have been used in host-guest chemistry, organic transformations[12], sensing, drug delivery,[13] as well as stabilizing reactive intermediates.[14] Specially, cavity induced stabilization of metastable states of different molecules[14h,14j,15] makes such architectures worthy candidates to study the host-guest interaction with spiropyran systems. Among several architectures that are reported with square planar Pd(II)/Pt(II),[16] molecular barrels are relatively less explored. The presence of two large open windows in a barrel may facilitate encapsulation or de-encapsulation of guest molecules.

Herein, we report the formation of two isomeric self-assembled Pd(II) barrels (**MB1** and **MB3**) upon 1:2 treatment of **L**[1] [benzene-1,4-di(4-terpyridine)] with *cis*-(tmeda)Pd(NO_3)$_2$ (**M**) in DMSO (Scheme 1). The symmetrical barrel **MB1** was obtained exclusively when the isolat-

ed mixture of barrels obtained from DMSO solution was heated in water. Presence of large cavity enabled us to carry out encapsulation of water insoluble organic guest molecules in the molecular pocket of **MB1**.

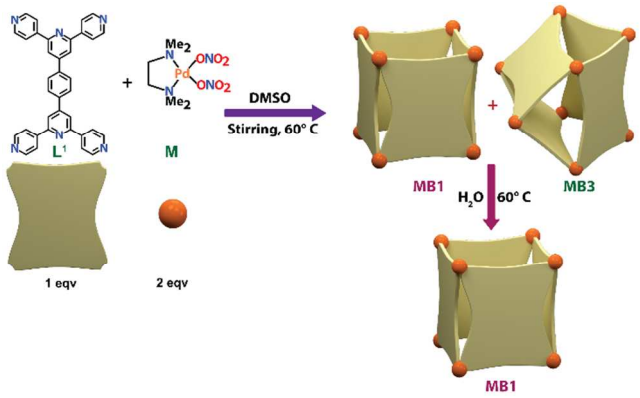

Scheme 1: Self-assembly of the molecular nano-barrel MB1 from tetrapyridyl ligand L¹ and M in 1:2 molar ratio.

Treatment of water insoluble bromo-spiropyran (**SP1**) with an aqueous solution of **MB1** produced a greenish blue solution due to the presence of merocyanine form (**MC1**) encapsulated into the hydrophobic cavity of **MB1** (Scheme 2). This coloured solution (**MC1⊂MB1**) was found to be stable under various stimuli such as visible light, UV light and heating over a long period due to stabilization of the transient **MC** form in confined pocket. Similar behaviour was also observed with a nitro substituted spiropyran (**SP2**). In this case, pink solution of the host-guest complex (**MC2⊂MB1**) was obtained and found to be stable under aforementioned stimuli. To explore the versatility of molecular barrel for stabilizing metastable **MC** forms, a similar study was performed using a tetraimidazole based molecular barrel (**MB2**)[17] which leads to the formation of an intense blue solution of **MC1⊂MB2**. The presence of wider windows causes a faster encapsulation of **MC1** by the barrel **MB2**. Though the transient **MC1** was stable in the confined pocket of **MB2** in visible light, heating of the solution showed reverse thermochromism as evident from sharp colour change from blue to colourless. Finally, the encapsulated **MC1** was successfully exchanged with polyaromatic hydrocarbons like pyrene, coronene and anthracene etc. which have higher binding ability with the host **MB2**. The encapsulation of **MC2** in **MB2** also produced an intense purple solution of (**MC2⊂MB2**), which was stable under external stimuli. Solid state transformation of **SP2** to its open **MC2** form upon UV-irradiation doesn't happen. However, in the presence of the barrels (**MB1** and **MB2**), we could successfully transform **SP2** to **MC2** and stabilize by arresting the metastable merocyanine form (**MC2**) even in solid state. Such stabilization of metastable merocyanine form of spiropyran compound both in solid and solution states using molecular barrels as safe containers is noteworthy. Unusual solid-state transformation of the colourless spiro form (**SP**) to the coloured merocyanine (**MC**) form and stabilization of the **MC** form were finally used for magic writing. Colourless hexane solution of **SP2** was used to write letters on a paper coated with the barrel **MB2** barrel. Invisible letters appeared as coloured letters upon exposure of the paper to sunlight/UV light due to solid state isomerization in presence of the barrel.

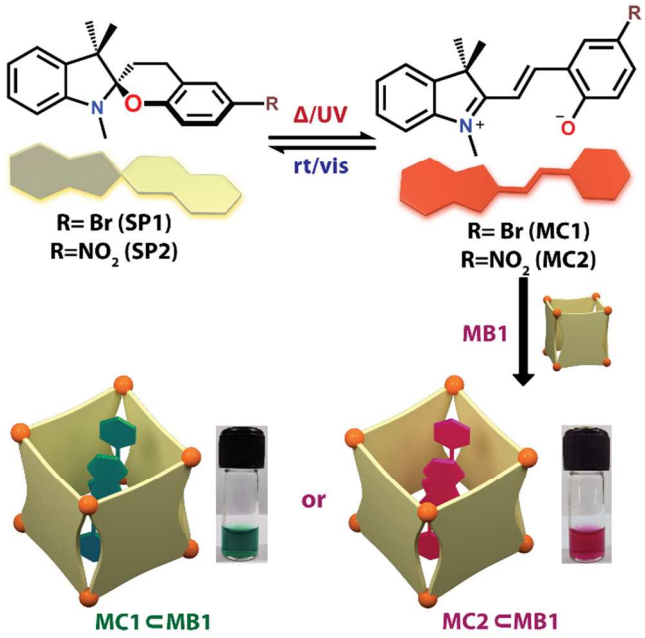

Scheme 2: Encapsulation of MC1 & MC2 into the cavity of nano-barrel MB1 to give greenish blue and pink solutions, respectively.

Results and Discussion:

The terpyridine based ligand **L¹** was synthesized following the literature procedure by treating terephthaldehyde with NaOH, 4-acetylpyridine and NH_4OH in ethanol.[18] Reaction of **L¹** with **M** in 2:1 molar ratio at 70° C overnight followed by treatment with excess ethyl acetate yielded off-white solid in quantitative yield. ^{1}H NMR spectra of this solid in DMSO-d_6 displayed multiple unassignable peaks at the aromatic region (Figure S3). However, this solid was soluble in water upon heating at 60° C. ^{1}H NMR spectrum of the product in D_2O at room temperature showed the presence of four peaks ranging from 9.24 to 7.84 ppm (Figure 1) due to **MB1**. Due to metal-ligand coordination significant downfield shifts for the pyridyl protons were noticed. All the aromatic protons were assigned with the help of ^{1}H-^{1}H COSY and ^{1}H-^{1}H NOESY NMR spectra (Figures S6,7). The peak position of proton (**b**) was observed at 8.53 ppm; however, with an integration value of four protons, which could be due to the presence of two different chemical environments of **b** because of a slower rotation than the NMR time scale of the pyridyl moiety in the final assembly. The ^{1}H-^{1}H COSY spectra (Figure S6) of the cage **MB1** indeed revealed the presence of two peaks for the **b** protons, the deshielded one residing close to the N atom has a δ value of 8.53 ppm and the shielded proton residing close to the **c** proton shows a δ value completely merging with that of **c** protons at 8.25 ppm. Therefore, a variable temperature ^{1}H NMR of **MB1** in D_2O was carried out in order to understand the behav-

iour of these protons (Figure 1). With increasing temperature, all the aromatic protons showed a gradual downfield shift; whereas, the peak at 8.53 ppm disappeared in between 40-50° C, and finally reappeared as a broad peak after 50° C and sharpening of this peak was observed with increasing temperature. Finally, ^{1}H-^{1}H COSY spectra at 80° C (Figure S8) revealed the presence of only one type of correlation between **a** and **b** protons. This variable temperature NMR study explains the presence of two non-equivalent protons for **b**.

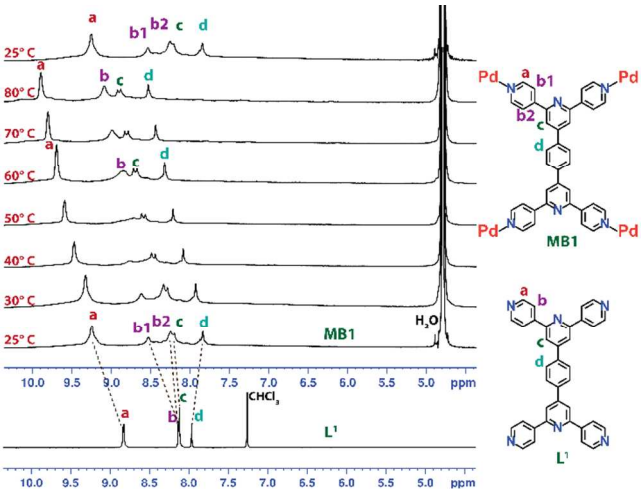

Figure 1: ^{1}H NMR spectra of the ligand **L^1** (bottom) in $CDCl_3$ and variable temperature ^{1}H NMR spectra of **MB1** in D_2O (top).

In order to record mass spectra, PF_6^- analogue of the nano-cage **MB1** was prepared by treating an aqueous solution of **MB1** with KPF_6 followed by separation of the white precipitate. The composition of the assembly was accurately ascertained by ESI-MS study in acetonitrile. The presence of several prominent peaks at m/z = 1107.87, 899.05, 749.89 and 638.17 with isotopic distribution patterns corresponding to $[\mathbf{MB1}\cdot 11PF_6^-]^{+5}$, $[\mathbf{MB1}\cdot 10PF_6^-]^{+6}$, and $[\mathbf{MB1}\cdot 9PF_6^-]^{+7}$ and $[\mathbf{MB1}\cdot 8PF_6^-]^{+8}$ charge fragments respectively, confirmed the formation of a $\mathbf{M_8L^1_4}$ species (Figure S9). Although, the proton NMR and ESI-MS spectroscopy specifically established the formation of a molecular barrel, further insight about the specific geometry of **MB1** was necessary to understand the dimension of the cavity. Several attempts to obtain single crystals of the nitrate analogue of **MB1** remained unsuccessful. However, single crystals of the PF_6^- analogue of **MB1** were successfully grown from slow vapour diffusion of dioxane and THF into a concentrated DMSO solution of **MB1** (Figure S4). Surprisingly, the presence of two different shaped crystals was observed from the THF diffusion set having different unit cell parameters. However, in case of the dioxane diffusion set only one type of crystals was observed having similar cell parameters to one of the crystal obtained from the THF diffusion set. The single crystal XRD data analysis of the dioxane diffused crystals unambiguously confirmed the formation of a tetrafacial barrel type architecture (Figure 2). Nonetheless, XRD analysis of the crystal having different cell parameters from the THF diffusion displayed the presence of isomeric structure **MB3**. **MB1** crystallizes in triclinic system with the space group *P*-1, containing one molecule in the unit cell located about a center of symmetry (the asymmetric unit corresponding to half of the molecule). With a single type of binding mode of **L^1**-Pd(II), two different shaped windows were formed containing two and four Pd(II) units. The open windows formed by four Pd atoms of the tetrafacial barrel **MB1** have a slight distortion in shape which is about 5° from the perfect square. This produces a rhombus like geometry of the open faces where the Pd-Pd-Pd angles are 85° and 95° with diagonal Pd-Pd distances of 17.17 Å and 18.84 Å, respectively (Figure 2). Both PF_6^- and NO_3^- anions were located in the crystal structure with different disordered solvent molecules including DMSO. All the counter-anions are present outside the barrel along with DMSO.

MB3 also was crystallized in *P*-1 with a single molecule in the asymmetric unit and thus with two molecules in the unit cell. **MB3** has a distorted barrel shaped geometry with different binding modes of **L^1** unlike in **MB1**. In contrast to **MB1**, two narrow windows containing two Pd(II) units and four wider windows containing three Pd(II) units with slight distortion of the faces were observed making the cage less symmetric. This particular assembly resembles with a geometry named Gyrobifastigium type solid J_{26} (Johnson solids)[19]. Having regular but not uniform faces makes this polyhedra very unique and rare in the literature[20]. Formation of these two different geometries in the DMSO solution makes the ^{1}H NMR spectra very complicated (Figure S3). However, the presence of two phenyl peaks at 8.19 ppm confirms the formation of two distinct geometries. In case of D_2O the fairly simple ^{1}H NMR spectra having distinct peaks in the aromatic region confirms the formation of highly symmetrical **MB1**. The formation of the symmetrical barrel in aqueous medium was also asserted from single point energy calculations of **MB1** and **MB3**, where the total energy of the asymmetric cage **MB3** is much higher than the symmetric isomer **MB1** (Table S2). However, presence of slight asymmetry in **MB1** causes the ^{1}H NMR peaks in the aromatic region to be broader. In addition, the spectrum shows split peaks at 8.25 ppm for the **c** protons, which remain such throughout the whole experimental temperature range.

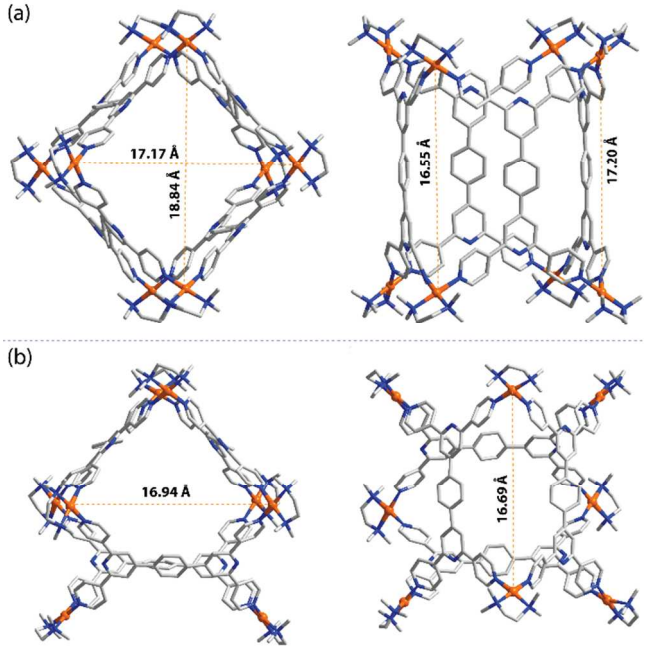

Figure 2: (a) Capped stick model of the single crystal XRD structure of the tetrafacial barrel **MB1**. (Left; Top view and right; side view. (b) Capped stick model of the single crystal XRD structure of the asymmetric barrel **MB3**. Colour codes: grey= carbon, blue= nitrogen and brown= palladium. (Hydrogen atoms, counter anions, solvent molecules and the disordered phenyl rings were omitted for better clarity).

The presence of two open windows associated with a huge barrel shaped hydrophobic cavity with a dimension of (12.7 Å×17.2 Å) makes **MB1** a potential candidate for encapsulation of water insoluble guest molecules of different shape and size. The photochromic bromo-spiropyran (**SP**)[22] was then used as guest. This bromo-spiropyran is colourless, soluble in common organic solvents, and stable under visible light. Upon irradiation with UV-light or heating at high temperature, the spiro-form converts to metastable coloured merocyanine form in solution phase (Scheme 2, *direct photochromism*). The metastable merocyanine form (**MC**) readily reverts back to colourless spiro-form (**SP**) under visible light or cooling to room temperature.

Stunningly, when a light-yellow solution of the nano-barrel **MB1** in D_2O was treated with excess amount of water insoluble solid bromo-spiropyran (**SP1**), the colour of the solution gradually turned into greenish blue within 5 hours and the colour got darker over a time period of 6 hours. UV/Vis spectra of the coloured solution exhibited a broad peak centered at around 590 nm. Generally, the planar open form (**MC1**) of bromo-spiropyran shows absorption peaks at around 520 and 550 nm in chloroform (Figure S13). Although, **SP1** is very poorly soluble in water and cannot be detected by ^{1}H NMR spectroscopy, overnight stirring of the organic guest in water produced an UV-Vis spectrum where the absorption bands are present only in the UV region (200-350 nm, Figure S12). Therefore, the new peak generated in the host-guest complex at 590 nm originates due to the presence of open **MC1** form. The solution remains coloured over several weeks under visible light. This result indicates that the barrel **MB1** can act as a safe container to arrest and stabilize the metastable merocyanine conformation (**MC1**).

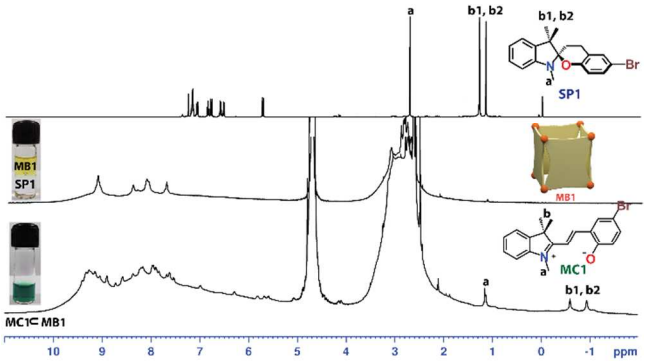

Figure 3: ^{1}H NMR spectra of **MC1⊂MB1** (bottom) in D_2O. ^{1}H NMR spectra of **MB1** (middle) in D_2O and **SP1** (top) in $CDCl_3$ after extraction with chloroform.

Finally, ^{1}H NMR spectra of that solution confirmed the formation of a host-guest complex (**MC⊂MB1**) exhibiting a complicated spectrum in contrast with the clearer ^{1}H NMR spectra of the host **MB1** (Figure 3). Multiple peaks appeared in the aromatic region presumably due to the lack of sufficient symmetry in the final host-guest complex. Along with these complex multiple aromatic peaks, several discrete broad peaks for the guest molecule were observed from 7.08 to -0.84 ppm. ^{1}H DOSY NMR confirmed the formation of a single host-guest component by displaying similar diffusion coefficient for the host and guest peaks. The high upfield shift of the aromatic as well as of methyl protons is due to a binding with the host molecule. The stability of cage **MB1** as well as of guest (**SP1**) was checked by extracting an aqueous solution of **MC1⊂MB1** with $CHCl_3$, which transformed the greenish blue solution into a light-yellow solution. Further investigation (Figure 3) on these two layers reveals that the water fraction contains **MB1** and chloroform part contains bromo-spiropyran (**SP** form). So, if the guest is taken out of the barrel, it exists in stable spiro (**SP**) form. The stoichiometry of the host-guest complex was determined as 1:2 (host : guest) from the ratio of integration values between host and guest peaks of the ^{1}H NMR spectra (Figure S16). This value was reasserted by extracting the guest molecule (**SP1**) with chloroform and removing the solvent to get solid **SP1** followed by determination of molar equivalent by simply weighing the sample, which also confirmed the formation of a 1:2 (host : guest) complex (Table S3). This result was supported by the presence of two peaks at -0.49 and -0.83 ppm for the dimethyl protons (in host-guest complex), which otherwise have equivalent chemical environment in the **MC1** form (Figures S18, 19).

Multiple attempts to grow single crystals of **MC1⊂MB1**by conventional slow evaporation and vapour diffusion technique were unsuccessful as the guest molecule comes out to the organic phase due to higher solubility in organic solvent/s. Nevertheless, the geometry of the

complex **MC1⊂MB1** was optimized by semi-empirical method by placing two **MC1** molecules as an ion pair (head to tell) into the cavity of the nano-barrel **MB1** (Figure 4). Finally, to understand the optical property, time dependent DFT calculation was carried out on this energy optimized structure, which resulted an UV/Vis spectrum having a λ_{max} (585 nm) value very close to the experimental one (Figure 4).

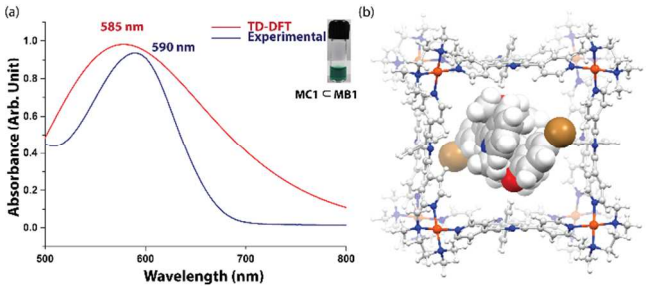

Figure 4: (a) Comparison of experimental and theoretical (TD-DFT) UV/Vis spectra. (b) Energy optimized geometry of **MC1⊂MB1.**

Interestingly, this host-guest complex **MC1⊂MB1** was stable under visible light for several weeks. Irradiation with UV light did not alter the colour and the ^{1}H NMR spectrum of the complex. Finally, the thermal stability of **MC1⊂MB1** was ensured by heating an aqueous solution of the complex at 50° C. The complex was stable for 6 hours under heating, as confirmed by ^{1}H NMR spectra (Figure S20). Similar stabilization of the merocyanine form by using nano-cavity in solution state was attempted by Zhou et al.[21] where β-CD was used as a molecular host. However, comparatively narrower cavity than **MB1** did not actually allow the open form to encapsulate into the cavity and therefore an alkyl substituted **SP** molecule was designed. Finally, the open form was stabilized by the encapsulation of the alkyl moiety of the closed form into the pocket followed by photo irradiation.

Next, we wanted to explore the possibility of encapsulation of nitro-spiropyran (**SP2**), which has larger nitro substituent. The close form (**SP2**) is stable in aprotic solvents. Irradiating with UV/sunlight produces blue open form (**MC2**) which reversibly transforms to the closed **SP2** in a few seconds in visible light. When the light-yellow powder of **SP2** was treated with an aqueous solution of **MB1**, formation of a pink solution was noticed after 6 h. The solution was characterized in the same way to find the formation of **MC2⊂MB1**. The ^{1}H NMR spectrum displayed a complicated spectrum with the dimethyl peaks (**b**) at -0.87 and -0.71 ppm (Figure S22). The stability of the nitro-spiropyran was checked by extracting the pink solution with chloroform. Both the layers (aqueous and organic) were characterized by ^{1}H NMR spectroscopy that resulted in spectra similar to the as-synthesized ones. Interestingly, during the extraction process the pink aqueous layer started to become light-yellow due to the presence of **MB1** whereas the chloroform layer initially appeared blue due to **MC2**, which converted to colourless **SP2** in a few seconds. This certainly explains that the open **MC2** form is encapsulated and it de-encapsulates from the cage after addition of an organic solvent such as chloroform and showing a blue colour. Following the previously described procedure the **MB1**:**MC2** stoichiometry was calculated to be 1:2. The geometry was optimized following the previously described method, which resulted in a similar structure (Table S2). TD-DFT study also provided UV/Vis absorption value (545 nm) very close to the experimental (549 nm) one. Thus, the container **MB1** could capture and stabilize the meta-stable form (**MC1/2**) of spiropyrans by means of encapsulation in its cavity (Figure S23).

To test if this unusual trapping of merocyanine form is possible by other molecular barrels, we performed similar study with a different molecular barrel (**MB2**)[17] that was designed employing a carbazole based tetraimidazole ligand. Interestingly, when a colourless aqueous solution of **MB2** was treated with excess of solid powder of hydrophobic bromo-spiropyran (**SP1**), the colour of the solution gradually turned blue within one hour. The colour got saturated over a time of three hours under visible light at room temperature. ^{1}H NMR of this blue solution showed that the hydrophobic spiropyran molecule was encapsulated inside the molecular barrel **MB2** and ^{1}H DOSY NMR confirmed the formation of a single component (Figure S37). Similar to **MB1**, when this aqueous blue solution is treated with a little amount chloroform and stirred for 10 min at room temperature, it gave a colourless bilayer of chloroform and water. Finally, ^{1}H NMR and its UV-Vis spectrum (Figures S27, S28) confirm that after extraction of the guest compound from the encapsulated blue solution, it is chemically intact. Subsequently, the aqueous blue solution was analysed by UV-Vis spectroscopy to confirm the nature of the encapsulated guest bromo-spiropyran. As can be seen from the UV-Vis absorption spectra (Figure 5), a new absorption peak at 600 nm appeared.

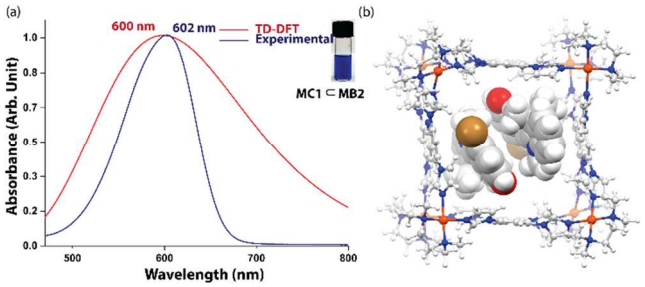

Figure 5: (a) Comparison of experimental and theoretical (TD-DFT) UV/Vis spectra. (b) Energy optimized geometry of **MC1⊂MB2.**

The geometry of the complex **MC1⊂MB2** was optimized (Figure 5) similarly as in the case of **MC1⊂MB1** (Figure 4). Finally, time dependent DFT calculation was carried out to get the energy optimized structure. The resulted UV-Vis spectrum exhibits a λ_{max} at 600 nm which is very close to the experimental one (Figure 5a).

Interestingly, heating the blue aqueous solution of **MC1⊂MB2** for 1.5 h at 60°C resulted in gradual decrease in blue colour which turns to colourless along with some

insoluble materials at the bottom. The ^{1}H NMR analysis showed that the aqueous solution contains the free host, whereas the insoluble material was bromo-spiropyran in stable **SP1** form, which was established by ^{1}H NMR analysis. Moreover, the absorption spectra of the aqueous solution and insoluble material confirmed that they contain **MB2** and bromo-spiropyran (**SP1** form), respectively.

Upon heating, the **MC1** comes out of the barrel in the form of **SP1** as insoluble solid. This colourless solution turns again blue upon keeping for a while under room light at ambient temperature because **SP1** is encapsulated in the barrel **MB2** in the form of **MC1**. So, we observed reverse thermochromism in presence of molecular barrel **MB2**.

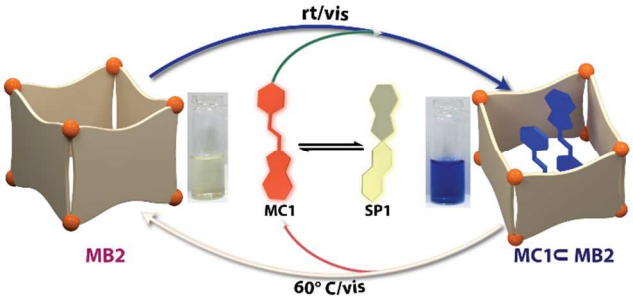

Figure 6: Schematic representation of reverse thermochromism of **MC1⊂MB2.**

A similar study was carried out with **SP2**, which resulted in a purple solution of the host-guest complex **MC2⊂MB2.** This was characterized by UV-Vis and ^{1}H NMR. A broad peak around 598 nm in UV-Vis spectra was observed. ^{1}H NMR spectrum displayed the usual complicated peaks in the aromatic region with the dimethyl peaks (**b**) shifted to -0.48 ppm, while for **MC1⊂MB2** it appears at around 0.0 ppm. This extra deshielding of the **b** protons evidently suggests a better binding with the host molecule for **MC2** than **MC1**. The stoichiometry was evaluated to be 1:2 (H:G) following similar procedure described earlier above (Table S3). However, crystal structure could not be obtained for this complex either. Therefore, the geometry was optimized according to the previously described method followed by TD-DFT calculation to get the UV/VIS spectra, which displayed a λ_{max} value (558 nm) very close to the experimental one (558 nm). In contrast to **MC1⊂MB2,** this complex was stable even after heating the solution at 50° C. Thus, **MC2⊂MB2** did not show any reverse thermochromism, which can be explained in terms of a better binding of **MC2** with **MB2** as explained from ^{1}H NMR spectra.

These ambiguity in stability of the host-guest complexes can be explained in terms of the cavity size of the respective molecular barrels. As it was observed, **MB1** takes a longer time to form the host-guest complex because of the presence of narrower windows with a cavity of larger length with respect to **MB2**, which comprises wider windows containing a cavity of smaller length. This makes a significant difference in binding capacity of **MB1** and **MB2** with **MC1**. ^{1}H NMR of **MC1⊂MB1** reflects highly deshielded peaks specially for proton **b** that appears at -0.84 ppm compared to **MC1⊂MB2**, where it appears at around 0.0 ppm. Therefore, it can be concluded that **MC1⊂MB1** is more stable than **MC1⊂MB2** and does not show any reverse thermochromism.

The rate of encapsulation was very slow in dark. The rate became fast in daylight and faster in sunlight. From this it can be concluded that in order to form the host-guest complex, the formation of the **MC** isomer is necessary and this can be facilitated by UV light. To confirm this idea, the encapsulation was carried out under UV light, which reduced the saturation time from 6 h to 0.5 h. These observations encouraged us to carry out the encapsulation reaction in solid state. To achieve this, **MB1** was thoroughly mixed with a concentrated THF solution of **SP2** and then dried to make a paste followed by UV (365 nm) irradiation. This resulted in the formation of a solid showing a slow pinkish luminescence over time which suggested the formation of the host-guest complex (**MC2⊂MB1**). After continuing the irradiation for 12 h the solid mixture turned into a pinkish colour. Finally, the resulted solid was characterized in D_2O by ^{1}H NMR, which exactly matches with the NMR observed from the solution phase study. To generalize this phenomenon, similar set of study was carried out with **MB2** which produced a deep purple solid having similar spectroscopic results to that of solution phase (Supporting Information: Video_**MB2**, Figure S40). Although, a solvent was introduced to make the paste, the question arises if that solvent has any role in the encapsulation? To confirm this, similar experiments were conducted using both the solids (**MB1/2** and **SP2**). Solid host and guest were mixed thoroughly by grinding the mixture followed by irradiation with UV (365 nm) light which also resulted in the host-guest formation as described before (Supporting Information: Video_SP2in**MB2**). This experiment unequivocally confirms the formation of host-guest complex in solid phase triggered by UV irradiation. Spiropyrans were previously incorporated into different solid matrixes such as nano particles[22], silica[23], polymers and also MOFs[24] by the help of either chemical bond formation or vapour-phase encapsulation technique. However, the solid state encapsulation by simple grinding in the present study including stabilization of transient merocyanine form in solid state is noteworthy. This exciting new finding motivated us to employ this system to develop a magic ink which could be used to write on a paper coated with molecular barrel. To do this, a filter paper was soaked in an aqueous solution of **MB2** followed by drying with hot air gun. Concomitantly colourless hexane solution of **SP2** was used as an invisible ink, which was poured into a fountain pen for writing purpose. As expected, the letters were invisible after writing with the ink (Figure 7) under room light, but when this filter paper kept under sunlight/UV for a few minutes, the coloured letters started to become visible (Figure 7) and were stable for several weeks. Interestingly, the letters could be erased by washing the paper thoroughly with CH_2Cl_2, which removes the encapsulated **MC2** from the host molecule to return the blank paper

containing only **MB2**. Finally, the recovered blank paper was again used to write with the invisible ink. This idea can be used to make a re-writeable paper.

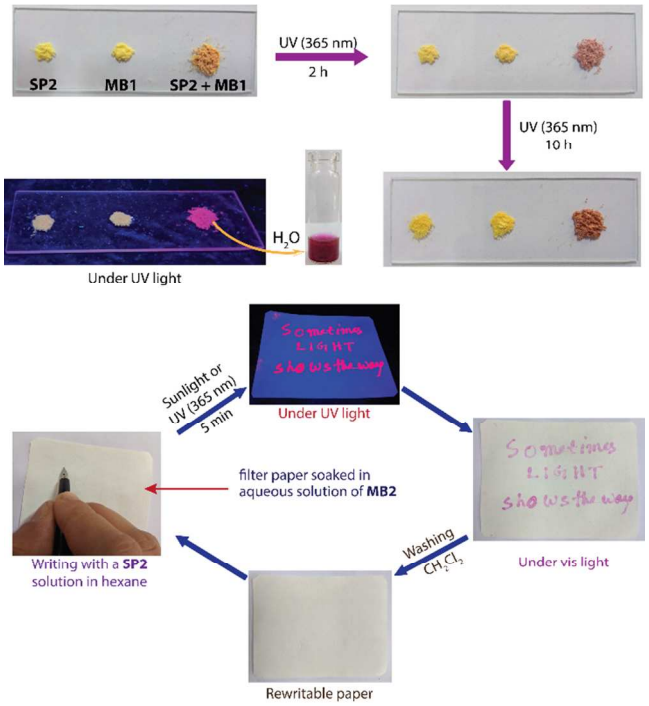

Figure 7: Encapsulation of **MC2** in **MB1** in solid phase (top). Writing with hexane solution of **SP2** on a filter paper soaked with aqueous solution of **MB2**, which can be used as a re-writable paper.

Conclusions:

In conclusion, self-assembly of a 90° Pd(II) acceptor **M** with terpyridine based tetra-pyridyl donors **L¹** in 2:1 molar ratio yielded two isometric molecular nano-barrels **MB1** and **MB3** in DMSO. A single assembly (**MB1**) was obtained by heating the mixture of barrels in aqueous medium. Spiropyran based compounds are generally stable in closed spiro-form (**SP**) in visible light and readily converts to transient merocyanine (**MC**) form upon UV irradiation or strong heating in solution phase. The transient **MC** form readily converts back again to stable spiro-form in visible light. However, such structural transformation of photochromic/thermochromic spiropyrans in solid state is very challenging for practical application. The molecular barrel **MB1** was found to stabilize the transient merocyanine form **MC1** of a bromo-spiropyran **SP1** when the aqueous solution of the barrel was treated with solid **SP1**. This host-guest complex **MC1⊂MB1** was found to be very stable under different external stimuli such as visible/UV-light and heating. The same barrel was also found to stabilize transient merocyanine isomer (**MC2**) of a nitro substituted spiropyran **SP2** in the form of a host-guest complex **MC2⊂MB1** in aqueous medium. Finally, to explore this unusual stabilization of transient merocyanine form of spiropyrans in the confined space of other molecular barrel, a similar study was carried out with a carbazole based tetrafacial molecular barrel **MB2**.[15] Treatment of **SP1** and **SP2** with aqueous solution of **MB2** produced blue and deep-purple solutions of host-guest complexes **MC1⊂MB2** and **MC2⊂MB2**, respectively. Although, the complex **MC2⊂MB2** was stable under different stimuli, the blue complex **MC1⊂MB2** showed a gradual decolouration upon heating due to de-encapsulation of the guest molecule from the barrel and transformed to the stable closed form **SP1**. Thus, **SP1** showed unique reverse thermochromism in presence of the barrel **MB2**. Such unusual stabilization of transient merocyanine form in visible light in confined space of molecular barrels was not only restricted to solution phase. Even solid mixture of the barrel (**MB1/2**) and spiro compound (**SP2**) upon irradiation with UV light produced merocyanine forms that were stable in solid state for very long period in visible light. The remarkable solid-state stabilization of the merocyanine in barrel was finally used for magic writing. A colourless hexane solution of **SP2** was used as invisible ink on a paper that was coated with **MB2**. The invisible letters appeared coloured upon keeping under UV/sunlight light for a few minutes due to the solid-state isomerization of the **SP2** to coloured **MC2** in solid state.

Experimental Section:

Methods and Materials:

Reagents used in this study were purchased from commercial sources and used without any purification. NMR studies were performed using a Bruker-make 400 MHz spectrometer and the chemical shifts (δ) in the spectra are reported in ppm relative to tetramethylsilane (Me_4Si) as an internal standard (0.0 ppm) or proton resonance resulting from incomplete deuteration of the solvents $(CD_3)_2SO$ (2.50 ppm), $CDCl_3$ (7.26 ppm) and D_2O (4.79 ppm). Electrospray ionization mass spectrometric (ESI-MS) analyses were carried out on an Agilent 6538 Ultra-High Definition (UHD) Accurate Mass Q-TOF spectrometer. The nano-barrel **MB2**[17], **SP1**[25] and **SP2**[26] were synthesized according to the reported procedure.

Synthesis of the Ligand L¹:

The ligand **L¹** was synthesized following reported procedure of terpyridine synthesis.[16] Terepthaldehyde (670 mg, 5 mmol) was taken into a flame dried 500 mL round bottom flask containing 50 mL of ethanol at 0° C followed by addition of NaOH (400 mg, 10 mmol) with stirring. To this cold solution 4-acetyl pyridine (2.42 g, 20 mmol) in 10 mL of ethanol was added dropwise. Finally, 60 mL of ammonia solution was added followed by stirring at 0° C for 1 h. The solution was then allowed to reach to room temperature and refluxed at 80°C for 24 h. Precipitate formed after refluxing was filtered and washed thoroughly with ethanol and water to get solid powder of **L¹** as pure product. Yield 1.5 g (55 %). %). ^{1}H NMR (400 MHz, $CDCl_3$): δ = 8.84 (d, 8H), 8.14 (m, 12H), 7.96 (s, 4H).

Synthesis of the Barrel MB1:

cis-(tmen)$Pd(NO_3)_2$ (**M**) (69.2 mg, 0.200 mmol) was dissolved in 3 mL DMSO and the yellow clear solution was added to the solid ligand **L¹** (54 mg, 0.100 mmol) and heated at 60 °C with stirring for 6 h resulting in clear brownish solution. The clear solution was then treated with 20 mL ethyl acetate to obtain light yellow precipitate

which was collected by filtration followed by washing with acetone and ether. It was then dried under vacuum and dissolved in D_2O by heating at 60° C for 10 minutes to record ^1H NMR spectra. Isolated yield: 110 mg (89%). ^1H NMR (400 MHz, D_2O) δ (ppm): 9.24 (broad s, 8H), 8.53 (broad s, 4H), 8.25 (m, 8H), 7.84 (s, 4H).

Preparation of MC1/2⊂MB1:

Barrel **MB1** (20.0 mg, 0.04 mmol) was dissolved in 1.5 mL of water by heating at 60° C to get a light-yellow solution. Solid powder of **SP1/2** (10.0 mg) was added to this solution and stirred at room temperature for 6 h to get greenish blue and pink solutions of the host-guest complexes **MC1⊂MB1** and **MC2⊂MB1**, respectively.

Preparation of MC1/2⊂MB 2:

Barrel **MB2** (18.2 mg, 0.04 mmol) was dissolved in 1.5 mL of water and to this solution solid powder of **SP1/2** (10.0 mg) was added and stirred at room temperature for 3 h to get blue and purple coloured solutions of the host-guest complexes **MC1⊂MB 2** and **MC1⊂MB 2**, respectively**.**

Solid State Encapsulations:

Respective barrel **MB1/2** (0.02 mmol) was mixed with **SP2** followed by through grinding. The mixture was then irradiated with UV light (365 nm), which resulted in a reddish fluorescence of the mixture. Over time the fluorescence got intensified and the colour changed from light-yellow to pink and finally deep purple.

Computational Calculation:

To understand the geometry of the host-guest complexes theoretical calculations were carried out by taking the 1:2 stoichiometry of the host-guest and the zwitterionic nature of the **MC** form into account. To obtain maximum symmetry two molecules of **MC** were arranged into the cavity of the barrels as an ion pair (head to tail) to avoid steric hindrance between the methyl groups. Then the geometry was optimized by semi-empirical method with PM6 basis set. Finally, time dependent DFT calculations were carried out on the optimized geometry by B3LYP method with a mixed basis set of 631g and lanl2dz. The resulted peaks in UV-Vis spectra from calculations have very close value/s with the experimental ones.

ASSOCIATED CONTENT

Additional NMR, UV-Vis, SCXRD parameters and ESI-MS spectra. "This material is available free of charge via the Internet at http://pubs.acs.org."

AUTHOR INFORMATION

Corresponding Author

* psm@ipc.iisc.ernet.in (P. S. Mukherjee)

ACKNOWLEDGMENT

P.S.M. thanks the Science and Engineering Research Board (New Delhi) for a research grant [Grant No. EMR/2015/002353]. P. H. thanks Milan Kumar Hazra for meaningful discussion about computational studies.

REFERENCES

(1) Stevens, M.; Merilaita, S. *Philosophical Transactions of the Royal Society B: Biological Sciences* **2009**, *364*, 423.
(2) Wald, G. *Nature* **1934**, *134*, 65.
(3) Feringa, B. L.; Jager, W. F.; de Lange, B. *Tetrahedron* **1993**, *49*, 8267-8310.
(4) (a)Kompa, K. L.; Levine, R. D. *Proc. Natl. Acad. Sci.* **2001**, *98*, 410; (b)Lukas, A. S.; Bushard, P. J.; Wasielewski, M. R. *J. Am. Chem. Soc.* **2001**, *123*, 2440-2441; (c)Balzani, V.; Credi, A.; Venturi, M. *ChemPhysChem* **2003**, *4*, 49-59; (d)Irie, M. *Chem. Rev.* **2000**, *100*, 1683-1684; (e)Irie, M. *Chem. Rev.* **2000**, *100*, 1685-1716.
(5) (a)Yamada, M.; Kondo, M.; Mamiya, J.-i.; Yu, Y.; Kinoshita, M.; Barrett, C. J.; Ikeda, T. *Angew. Chem. Int. Ed.* **2008**, *47*, 4986-4988; (b)Chovnik, O.; Balgley, R.; Goldman, J. R.; Klajn, R. *J. Am. Chem. Soc.* **2012**, *134*, 19564-19567; (c)Klajn, R.; Bishop, K. J. M.; Fialkowski, M.; Paszewski, M.; Campbell, C. J.; Gray, T. P.; Grzybowski, B. A. *Science* **2007**, *316*, 261; (d)Das, S.; Ranjan, P.; Maiti, P. S.; Singh, G.; Leitus, G.; Klajn, R. *Adv. Mater.* **2013**, *25*, 422-426.
(6) (a)Bandara, H. M. D.; Burdette, S. C. *Chem. Soc. Rev.* **2012**, *41*, 1809-1825; (b)Henzl, J.; Mehlhorn, M.; Gawronski, H.; Rieder, K.-H.; Morgenstern, K. *Angew. Chem. Int. Ed.* **2006**, *45*, 603-606; (c)Zhang, J.; Whitesell, J. K.; Fox, M. A. *Chem. Mater.* **2001**, *13*, 2323-2331; (d)Minkin, V. I. *Chem. Rev.* **2004**, *104*, 2751-2776; (e)Berkovic, G.; Krongauz, V.; Weiss, V. *Chem. Rev.* **2000**, *100*, 1741-1754; (f)Kudernac, T.; van der Molen, S. J.; van Wees, B. J.; Feringa, B. L. *Chem. Commun.* **2006**, 3597-3599; (g)Heinz, B.; Malkmus, S.; Laimgruber, S.; Dietrich, S.; Schulz, C.; Rück-Braun, K.; Braun, M.; Zinth, W.; Gilch, P. *J. Am. Chem. Soc.* **2007**, *129*, 8577-8584; (h)Ohara, K.; Inokuma, Y.; Fujita, M. *Angew. Chem. Int. Ed.* **2010**, *49*, 5507-5509.
(7) (a)Wohl, C. J.; Kuciauskas, D. *J. Phys. Chem. B* **2005**, *109*, 22186-22191; (b)Rini, M.; Holm, A.-K.; Nibbering, E. T. J.; Fidder, H. *J. Am. Chem. Soc.* **2003**, *125*, 3028-3034; (c)Hobley, J.; Malatesta, V.; Millini, R.; Montanari, L.; O Neil Parker, W.; Vincenzo Malatesta Roberto Millini Luciano Montanari Wallace O. Neil Parker, J. *PCCP* **1999**, *1*, 3259-3267; (d)Keum, S.-R.; Hur, M.-S.; Kazmaier, P. M.; Buncel, E. *Can. J. Chem.* **1991**, *69*, 1940-1947.
(8) (a)Day, J. H. *Chem. Rev.* **1963**, *63*, 65-80; (b)Byrne, R.; Fraser, K. J.; Izgorodina, E.; MacFarlane, D. R.; Forsyth, M.; Diamond, D. *PCCP* **2008**, *10*, 5919-5924.
(9) (a)Parthenopoulos, D. A.; Rentzepis, P. M. *Science* **1989**, *245*, 843; (b)Tomioka, H.; Itoh, T. *J. Chem. Soc., Chem. Commun.* **1991**, 532-533; (c)Casades, I.; Constantine, S.; Cardin, D.; García, H.; Gilbert, A.; Márquez, F. *Tetrahedron* **2000**, *56*, 6951-6956; (d)Kinashi, K.; Harada, Y.; Ueda, Y. *Thin Solid Films* **2008**, *516*, 2532-2536; (e)Renkecz, T.; Mistlberger, G.; Pawlak, M.; Horváth, V.; Bakker, E. *ACS Applied Materials & Interfaces* **2013**, *5*, 8537-8545; (f)Kundu, P. K.; Olsen, G. L.; Kiss, V.; Klajn, R. *Nat. Commun.* **2014**, *5*, 3588; (g)Zhang, F.; Zou, X.; Feng, W.; Zhao, X.; Jing, X.; Sun, F.; Ren, H.; Zhu, G. *J. Mater. Chem.* **2012**, *22*, 25019-25026; (h)Samanta, D.; Galaktionova, D.; Gemen, J.; Shimon, L. J. W.; Diskin-Posner, Y.; Avram, L.; Král, P.; Klajn, R. *Nat. Commun.* **2018**, *9*, 641.
(10) (a)Bloch, W. M.; Abe, Y.; Holstein, J. J.; Wandtke, C. M.; Dittrich, B.; Clever, G. H. *J. Am. Chem. Soc.* **2016**, *138*, 13750-13755; (b)Bogie, P. M.; Holloway, L. R.; Lyon, Y.; Onishi, N. C.; Beran, G. J. O.; Julian, R. R.; Hooley, R. J. *Inorg. Chem.* **2018**, *57*, 4155-4163; (c)Clever, G. H.; Punt, P. *Acc. Chem. Res.* **2017**, *50*, 2233-2243; (d)Cook, T. R.; Stang, P. J. *Chem. Rev.* **2015**, *115*, 7001-7045; (e)Frank, M.; Ahrens, J.; Bejenke, I.; Krick, M.; Schwarzer, D.; Clever, G. H. *J. Am. Chem. Soc.* **2016**, *138*, 8279-8287; (f)Hardy, M.; Struch, N.; Topić, F.; Schnakenburg, G.; Rissanen, K.; Lützen, A. *Inorg. Chem.* **2018**, *57*, 3507-3515; (g)Johnson, A.

M.; Young, M. C.; Zhang, X.; Julian, R. R.; Hooley, R. J. *J. Am. Chem. Soc.* **2013**, *135*, 17723-17726; (h)Percástegui, E. G.; Mosquera, J.; Nitschke, J. R. *Angew. Chem. Int. Ed.* **2017**, *56*, 9136-9140; (i)Saha, M. L.; Schmittel, M. *J. Am. Chem. Soc.* **2013**, *135*, 17743-17746; (j)Saha, M. L.; Schmittel, M. *Inorg. Chem.* **2016**, *55*, 12366-12375; (k)Struch, N.; Bannwarth, C.; Ronson, T. K.; Lorenz, Y.; Mienert, B.; Wagner, N.; Engeser, M.; Bill, E.; Puttreddy, R.; Rissanen, K.; Beck, J.; Grimme, S.; Nitschke, J. R.; Lützen, A. *Angew. Chem. Int. Ed.* **2017**, *56*; (l)Sun, Y.; Li, S.; Zhou, Z.; Saha, M. L.; Datta, S.; Zhang, M.; Yan, X.; Tian, D.; Wang, H.; Wang, L.; Li, X.; Liu, M.; Li, H.; Stang, P. J. *J. Am. Chem. Soc.* **2018**, *140*, 3257-3263; (m)Uchida, J.; Yoshio, M.; Sato, S.; Yokoyama, H.; Fujita, M.; Kato, T. *Angew. Chem. Int. Ed.* **2017**, *56*, 14085-14089; (n)Yue, Z.; Wang, H.; Li, Y.; Qin, Y.; Xu, L.; Bowers, D. J.; Gangoda, M.; Li, X.; Yang, H.-B.; Zheng, Y.-R. *Chem. Commun.* **2018**, *54*, 731-734; (o)Zhang, D.; Ronson, T. K.; Mosquera, J.; Martinez, A.; Guy, L.; Nitschke, J. R. *J. Am. Chem. Soc.* **2017**, *139*, 6574-6577; (p)Singh, N.; Singh, J.; Kim, D.; Kim, D. H.; Kim, E.-H.; Lah, M. S.; Chi, K.-W. *Inorg. Chem.* **2018**, *57*, 3521-3528; (q)Jo, J.-H.; Singh, N.; Kim, D.; Cho, S. M.; Mishra, A.; Kim, H.; Kang, S. C.; Chi, K.-W. *Inorg. Chem.* **2017**, *56*, 8430-8438; (r)Song, Y. H.; Singh, N.; Jung, J.; Kim, H.; Kim, E. H.; Cheong, H. K.; Kim, Y.; Chi, K. W. *Angew. Chem.* **2016**, *128*, 2047-2051; (s)Singh, N.; Jang, S.; Jo, J. H.; Kim, D. H.; Park, D. W.; Kim, I.; Kim, H.; Kang, S. C.; Chi, K. W. *Chem. Eur. J.* **2016**, *22*, 16157-16164; (t)Zhang, D.; Li, D.; Li, X.; Jin, W. *Dyes and Pigments* **2018**, *152*, 43-48; (u)Zhang, Y.; Zhou, Q.-F.; Huo, G.-F.; Yin, G.-Q.; Zhao, X.-L.; Jiang, B.; Tan, H.; Li, X.; Yang, H.-B. *Inorg. Chem.* **2018**, *57*, 3516-3520.

(11) (a)Fujita, M.; Tominaga, M.; Hori, A.; Therrien, B. *Acc. Chem. Res.* **2005**, *38*, 369-378; (b)Leininger, S.; Olenyuk, B.; Stang, P. J. *Chem. Rev.* **2000**, *100*, 853-908; (c)Mukherjee, S.; Mukherjee, P. S. *Chem. Commun.* **2014**, *50*, 2239-2248; (d)Northrop, B. H.; Zheng, Y.-R.; Chi, K.-W.; Stang, P. J. *Acc. Chem. Res.* **2009**, *42*, 1554-1563; (e)Saha, M. L.; Mittal, N.; Bats, J. W.; Schmittel, M. *Chem. Commun.* **2014**, *50*, 12189-12192; (f)Seidel, S. R.; Stang, P. J. *Acc. Chem. Res.* **2002**, *35*, 972-983; (g)Gütz, C.; Hovorka, R.; Schnakenburg, G.; Lützen, A. *Chem. Eur. J.* **2013**, *19*, 10890-10894; (h)Lützen, A. *Angew. Chem. Int. Ed.* **2005**, *44*, 1000-1002; (i)Ronson, T. K.; Zarra, S.; Black, S. P.; Nitschke, J. R. *Chem. Commun.* **2013**, *49*, 2476-2490; (j)Smulders, M. M. J.; Jiménez, A.; Nitschke, J. R. *Angew. Chem. Int. Ed.* **2012**, *51*, 6681-6685; (k)Weilandt, T.; Kiehne, U.; Schnakenburg, G.; Lutzen, A. *Chem. Commun.* **2009**, 2320-2322; (l)Bar, A. K.; Chakrabarty, R.; Mukherjee, P. S. *Inorg. Chem.* **2009**, *48*, 10880-10882; (m)Chakrabarty, R.; Mukherjee, P. S.; Stang, P. J. *Chem. Rev.* **2011**, *111*, 6810-6918; (n)Bhat, I. A.; Samanta, D.; Mukherjee, P. S. *J. Am. Chem. Soc.* **2015**, *137*, 9497-9502; (o)Sun, Q. F.; Murase, T.; Sato, S.; Fujita, M. *Angew. Chem. Int. Ed.* **2011**, *50*, 10318-10321; (p)Jiang, B.; Chen, L.-J.; Xu, L.; Liu, S.-Y.; Yang, H.-B. *Chem. Commun.* **2013**, *49*, 6977-6979; (q)Fujita, M. *Chem. Soc. Rev.* **1998**, *27*, 417-425; (r)Suzuki, K.; Takao, K.; Sato, S.; Fujita, M. *J. Am. Chem. Soc.* **2010**, *132*, 2544-2545; (s)Yan, L.-L.; Tan, C.-H.; Zhang, G.-L.; Zhou, L.-P.; Bünzli, J.-C.; Sun, Q.-F. *J. Am. Chem. Soc.* **2015**, *137*, 8550-8555; (t)Wood, C. S.; Ronson, T. K.; Belenguer, A. M.; Holstein, J. J.; Nitschke, J. R. *Nat. Chem.* **2015**, *7*, 354-358; (u)Hong, C. M.; Kaphan, D. M.; Bergman, R. G.; Raymond, K. N.; Toste, F. D. *J. Am. Chem. Soc.* **2017**, *139*, 8013-8021; (v)Yin, G.-Q.; Wang, H.; Wang, X.-Q.; Song, B.; Chen, L.-J.; Wang, L.; Hao, X.-Q.; Yang, H.-B.; Li, X. *Nat. Commun.* **2018**, *9*, 567; (w)Zhang, M.; Yin, S.; Zhang, J.; Zhou, Z.; Saha, M. L.; Lu, C.; Stang, P. J. *Proc. Natl. Acad. Sci.* **2017**, *114*, 3044; (x)Lee, H.; Elumalai, P.; Singh, N.; Kim, H.; Lee, S. U.; Chi, K.-W. *J. Am. Chem. Soc.* **2015**, *137*, 4674-4677.

(12) (a)Cai, L.-X.; Li, S.-C.; Yan, D.-N.; Zhou, L.-P.; Guo, F.; Sun, Q.-F. *J. Am. Chem. Soc.* **2018**, *140*, 4869-4876; (b)Oldacre, A. N.; Friedman, A. E.; Cook, T. R. *J. Am. Chem. Soc.* **2017**, *139*, 1424-1427; (c)Ueda, Y.; Ito, H.; Fujita, D.; Fujita, M. *J. Am. Chem. Soc.* **2017**, *139*, 6090-6093.

(13) (a)Yu, G.; Cook, T. R.; Li, Y.; Yan, X.; Wu, D.; Shao, L.; Shen, J.; Tang, G.; Huang, F.; Chen, X.; Stang, P. J. *Proc. Natl. Acad. Sci.* **2016**, *113*, 13720; (b)Yu, G.; Yu, W.; Mao, Z.; Gao, C.; Huang, F. *Small* **2015**, *11*, 919-925.

(14) (a)Mal, P.; Breiner, B.; Rissanen, K.; Nitschke, J. R. *Science* **2009**, *324*, 1697-1699; (b)Liu, Y.; Perez, L.; Mettry, M.; Easley, C. J.; Hooley, R. J.; Zhong, W. *J. Am. Chem. Soc.* **2016**, *138*, 10746-10749; (c)Kim, S.; Dawson, K. W.; Gelfand, B. S.; Taylor, J. M.; Shimizu, G. K. *J. Am. Chem. Soc.* **2013**, *135*, 963-966; (d)Howlader, P.; Das, P.; Zangrando, E.; Mukherjee, P. S. *J. Am. Chem. Soc* **2016**, *138*, 1668-1676; (e)Horike, S.; Umeyama, D.; Kitagawa, S. *Acc. Chem. Res.* **2013**, *46*, 2376-2384; (f)Murase, T.; Nishijima, Y.; Fujita, M. *J. Am. Chem. Soc.* **2011**, *134*, 162-164; (g)Rizzuto, F. J.; Wu, W.-Y.; Ronson, T. K.; Nitschke, J. R. *Angew. Chem. Int. Ed.* **2016**, *55*, 7958-7962; (h)Fiedler, D.; Bergman, R. G.; Raymond, K. N. *Angew. Chem. Int. Ed.* **2006**, *45*, 745-748; (i)Yoshizawa, M.; Tamura, M.; Fujita, M. *Science* **2006**, *312*, 251-254; (j)Takezawa, H.; Akiba, S.; Murase, T.; Fujita, M. *J. Am. Chem. Soc.* **2015**, *137*, 7043-7046.

(15) (a)Tashiro, S.; Kobayashi, M.; Fujita, M. *J. Am. Chem. Soc.* **2006**, *128*, 9280-9281; (b)Takezawa, H.; Murase, T.; Fujita, M. *J. Am. Chem. Soc.* **2012**, *134*, 17420-17423.

(16) (a)Roy, B.; Saha, R.; Ghosh, A. K.; Patil, Y.; Mukherjee, P. S. *Inorg. Chem.* **2017**, *56*, 3579-3588; (b)Li, K.; Zhang, L.-Y.; Yan, C.; Wei, S.-C.; Pan, M.; Zhang, L.; Su, C.-Y. *J. Am. Chem. Soc.* **2014**, *136*, 4456-4459; (c)Klein, C.; Gütz, C.; Bogner, M.; Topić, F.; Rissanen, K.; Lützen, A. *Angew. Chem. Int. Ed.* **2014**, *53*, 3739-3742; (d)Samanta, D.; Mukherjee, P. S. *Chem. Eur. J.* **2014**, *20*, 12483-12492; (e)Yan, Q.-Q.; Hu, S.-J.; Zhang, G.-L.; Zhang, T.; Zhou, L.-P.; Sun, Q.-F. *Molecules* **2018**, *23*, 363.

(17) Roy, B.; Ghosh, A. K.; Srivastava, S.; D'Silva, P.; Mukherjee, P. S. *J. Am. Chem. Soc.* **2015**, *137*, 11916-11919.

(18) (a)Liu, C.-L.; Zheng, C.-J.; Liu, X.-K.; Chen, Z.; Yang, J.-P.; Li, F.; Ou, X.-M.; Zhang, X.-H. *Journal of Materials Chemistry C* **2015**, *3*, 1068-1076; (b)Beddoe, S. V. F.; Fitzpatrick, A. J.; Price, J. R.; Mallo, N.; Beves, J. E.; Morgan, G. G.; Kitchen, J. A.; Keene, T. D. *Cryst. Growth Des.* **2017**, *17*, 6603-6612; (c)Constable, E. C.; Zhang, G.; Coronado, E.; Housecroft, C. E.; Neuburger, M. *CrystEngComm* **2010**, *12*, 2139-2145.

(19) Damasceno, P. F.; Engel, M.; Glotzer, S. C. *Science* **2012**, *337*, 453.

(20) (a)Cecot, G.; Marmier, M.; Geremia, S.; De Zorzi, R.; Vologzhanina, A. V.; Pattison, P.; Solari, E.; Fadaei Tirani, F.; Scopelliti, R.; Severin, K. *J. Am. Chem. Soc.* **2017**, *139*, 8371-8381; (b)Cecot, G.; Alameddine, B.; Prior, S.; Zorzi, R. D.; Geremia, S.; Scopelliti, R.; Fadaei, F. T.; Solari, E.; Severin, K. *Chem. Commun.* **2016**, *52*, 11243-11246.

(21) Zhou, J.; Sui, Q.; Huang, B. *J. Photochem. Photobiol., A* **1998**, *117*, 129-136.

(22) Klajn, R. *Chem. Soc. Rev.* **2014**, *43*, 148-184.

(23) (a)Parrot, A.; Izzet, G.; Chamoreau, L.-M.; Proust, A.; Oms, O.; Dolbecq, A.; Hakouk, K.; El Bekkachi, H.; Deniard, P.; Dessapt, R.; Mialane, P. *Inorg. Chem.* **2013**, *52*, 11156-11163; (b)Rosario, R.; Gust, D.; Hayes, M.; Jahnke, F.; Springer, J.; Garcia, A. A. *Langmuir* **2002**, *18*, 8062-8069.

(24) Schwartz, H. A.; Olthof, S.; Schaniel, D.; Meerholz, K.; Ruschewitz, U. *Inorg. Chem.* **2017**, *56*, 13100-13110.

(25) Qi, Q.; Qian, J.; Ma, S.; Xu, B.; Zhang, S. X. A.; Tian, W. *Chem. Eur. J.* **2015**, *21*, 1149-1155.

(26) (a)Breslin, V. M.; Garcia-Garibay, M. A. *Cryst. Growth Des.* **2017**, *17*, 637-642; (b)Balmond, E. I.; Tautges, B. K.; Faulkner, A. L.; Or, V. W.; Hodur, B. M.; Shaw, J. T.; Louie, A. Y. *J. Org. Chem.* **2016**, *81*, 8744-8758; (c)Udayabhaskararao, T.; Kundu, P. K.; Ahrens, J.; Klajn, R. *ChemPhysChem* **2016**, *17*, 1805-1809.

Self-Assembled Pd(II) Barrels as Containers for Transient Merocyanine form and Reverse Thermochromism of Spiropyran

Prodip Howlader,[a] Bijnaneswar Mondal,[a] Prioti Choudhury Purba,[a] Ennio Zangrando[b] and Partha Sarathi Mukherjee[a]*